

UNCLASSIFIED

AD NUMBER

AD850572

LIMITATION CHANGES

TO:

Approved for public release; distribution is unlimited.

FROM:

Distribution authorized to U.S. Gov't. agencies and their contractors;  
Administrative/Operational Use; 25 MAR 1969.  
Other requests shall be referred to Space and Missile Systems Organization (SMSO), Los Angeles, CA 90045-0000. This document contains export-controlled technical data.

AUTHORITY

SMSO per ltr, 28 Feb 1972

THIS PAGE IS UNCLASSIFIED

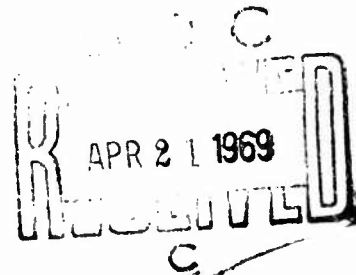
AD850572

## The Dynamic Response of Graphitic Materials

Prepared by A. E. SCHMIDT, JR.  
Materials Sciences Laboratory

69 MAR 25

Laboratory Operations  
AEROSPACE CORPORATION



Prepared for SPACE AND MISSILE SYSTEMS ORGANIZATION  
AIR FORCE SYSTEMS COMMAND  
LOS ANGELES AIR FORCE STATION  
Los Angeles, California, 90045  
*attn: SMSD*

THIS DOCUMENT IS SUBJECT TO SPECIAL EXPORT CONTROLS AND EACH TRANSMITTAL TO FOREIGN GOVERNMENTS OR FOREIGN NATIONALS MAY BE MADE ONLY WITH PRIOR APPROVAL OF SAMSO(SMPTM). THE DISTRIBUTION OF THIS REPORT IS LIMITED BECAUSE IT CONTAINS TECHNOLOGY RESTRICTED BY MUTUAL SECURITY ACTS.

Air Force Report No.  
SAMSO-TR-68-~~38~~-380

Aerospace Report No.  
TR-0200(4250-30)-2

THE DYNAMIC RESPONSE OF GRAPHITIC MATERIALS

Prepared by  
A. E. Schmidt, Jr.  
Materials Sciences Laboratory

69 MAR 25

Laboratory Operations  
AEROSPACE CORPORATION

Prepared for  
SPACE AND MISSILE SYSTEMS ORGANIZATION  
AIR FORCE SYSTEMS COMMAND  
LOS ANGELES AIR FORCE STATION  
Los Angeles, California

*attn: S.M.S.D*

This document is subject to special export controls and each transmittal to foreign governments or foreign nationals may be made only with prior approval of SAMSO (~~SECRET~~). The distribution of this report is limited because it contains technology restricted by mutual security acts.

## FOREWORD

This report, published by the Aerospace Corporation, El Segundo, California, under Air Force Contract F04701-68-C-0200, documents research carried out from October 1967 to March 1968.

The author wishes to express special thanks to J. H. Richardson, of the Metallurgy and Ceramics Department, for his assistance in the interpretation of test sample microstructural features.

This report was submitted on 21 August 1968 to Lt. Richard A. Binger, SMTTM, for review and approval.

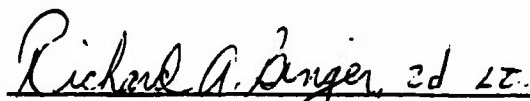
Approved



---

W. C. Riley, Director  
Materials Sciences Laboratory

Publication of this report does not constitute Air Force approval of the report's findings or conclusions. It is published only for the exchange and stimulation of ideas.



---

Richard A. Binger, 2nd Lt, USAF  
Project Officer

## ABSTRACT

Dynamic tensile properties of monolithic (ATJ, POCO (AXF), and Graphitite G) and pyrolytic graphite (PG, boron-doped PG, and hafnium-doped PG) have been obtained. In all cases, the dynamic tensile strength is 2 to 7 times the published values of static tensile strength. Material failure modes are similar to those observed for fracture under static loading conditions.

## CONTENTS

FOREWORD . . . . .	ii
ABSTRACT . . . . .	iii
I. INTRODUCTION . . . . .	1
II. THEORY . . . . .	3
A. Materials Background . . . . .	3
B. Shock Wave Propagation . . . . .	7
III. EXPERIMENTAL RESULTS . . . . .	11
IV. DISCUSSION . . . . .	17
V. CONCLUSIONS . . . . .	19
REFERENCES . . . . .	21

## FIGURES

1. Pretest Photomicrographs of Pyrolytic Graphite Materials . . . . .	4
2. Tension Wave Development . . . . .	8
3. Test Geometry . . . . .	12
4. Post-test Photomicrographs of Pyrolytic Graphite Materials . . . . .	13
5. Fracture Patterns . . . . .	14
6. Determination of Median Stress for Pyrolytic Graphite . . . . .	15

## TABLES

I.	Mechanical Properties of Graphitic Materials at Room Temperature. . . . .	6
II.	Fracture Stress of Graphitic Materials as Obtained from Impact Tests. . . . .	16
III.	Comparison of Static and Dynamic Tensile Strength. . . . .	18

## I. INTRODUCTION

Graphitic materials are receiving consideration for nose tip and heat shield application on advanced reentry vehicles because of their low ablation rate and high strength at elevated temperatures. In selecting materials for design application where impulsive loading is encountered, the dynamic response characteristics of the candidate materials must be known. The present investigation studies the response characteristics of pyrolytic and monolithic graphite: material failure modes, dynamic strength, and relative performance are included.

The materials under investigation are monolithic graphites (ATJ, POCO (AXF), and Graphitite G) and pyrolytic graphites (conventional PG, boron-doped PG, and hafnium-doped PG). Samples are subjected to strain rates of 200 to 2000 in/in/sec and peak stress wave amplitudes between 2000 and 30,000 psi. The results of this investigation have found immediate application in the evaluation of these materials in studies concerned with the simulation of certain weapon effects.

## II. THEORY

### A. MATERIALS BACKGROUND

Pyrolytic graphites are formed by vapor deposition techniques, resulting in a highly oriented, highly anisotropic material without a binder phase and having almost no porosity. The c-direction strength of the PG materials (i. e., across the oriented crystallite layers that are in the a-b plane) is both the lowest and generally the most critical in advanced reentry system applications. One approach to improving the c-direction strength is the introduction of boron, which may pin the crystallite layers together.

The pyrolytic graphites are expected to fail in tension by delamination between crystallite layers (i. e., in the c-direction) because of the highly oriented nature of the material. The growth and joining of microcracks is the most likely manifestation of this failure mode. The existence of microcracks in the various PG-based materials is evident from photomicrographs of laboratory control samples (Fig. 1) and is attributed to the manufacturing processes.

Monolithic graphites are made up of carbon crystallites in a carbon binder, generally a pitch-like material. A lining up or layering of the carbon crystallites along preferred directions is caused by the particular fabrication process employed; for example, ATJ is a molded graphite having a large fraction of the individual crystallites oriented in planes perpendicular to the molding axis. Graphitite G is an extruded graphite, and the majority of the crystallite planes are parallel to the extrusion axis. POCO graphite is reported to have an anisotropy of less than 3% and may be assumed to be isotropic for all practical purposes.

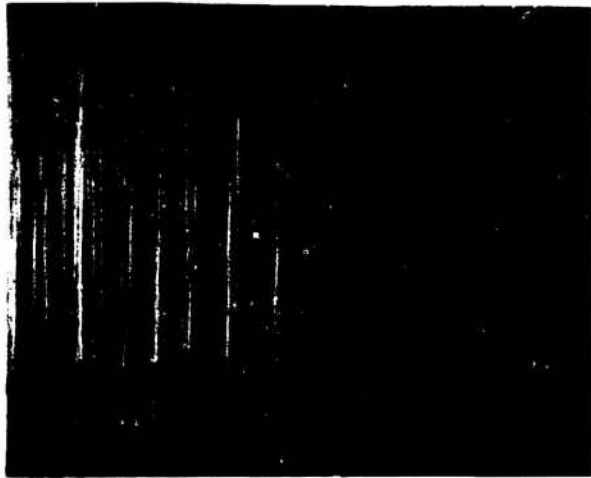
A study of deformation mechanisms in a typical monolithic graphite under static tensile and compression loading to failure (Ref. 1) showed extensive cracking between crystallites and parallel to the a-b direction. The hypothesis was advanced that cracking always tends to initiate in inter-layer directions and that cracks are propagated, by some type of interlayer



Pyrolytic graphite (PG).  
Taken  $\times 100$ ; shown  $\times 70$ .



Boron-doped PG (BPG).  
Taken  $\times 100$ ; shown  $\times 70$ .



Hafnium-doped PG (HPG).  
Taken  $\times 50$ ; shown  $\times 40$ .

Figure 1. Pretest Photomicrographs of Pyrolytic Graphite Materials. (c-direction is vertical.)

fracture mechanism, between imperfections that lie in planes parallel to the general trend of crystallite orientation. The imperfections could be pores or flaws that develop between crystallites during cool-down from the graphitization temperature. Under tensile loading, the cracks were perpendicular to the direction of the applied stress, but in compression the cracking was parallel to the applied stress. Thus, failure modes of the monolithic graphites under dynamic loading would be expected to be more complicated than for the PG materials, but should still be controlled primarily by the grain orientation and the direction of loading.

The mechanical properties of polycrystalline graphite materials depend on porosity, grain size, and crystallite orientation. Data presented in Ref. 2, for example, show a significant difference in Young's modulus and ultimate strengths for loading "with the grain" and "against the grain" for a number of graphitic materials. Similar data for additional materials are given in Refs. 3 and 4. The effect of porosity on the mechanical properties of isotropic graphites is discussed in Ref. 5 and is shown to be a significant factor in material properties. The physical properties of the materials studied in this program are summarized in Table I.

Data presented in Ref. 2 also indicate differences in material response depending on whether the loading is tensile or compressive, and that, under either loading condition, the stress-strain curve is nonlinear. Therefore, caution must be exercised in employing published material property values that do not specify the appropriate conditions of grain orientation, loading direction, and whether tensile or compressive loading was used. The speed with which a stress disturbance will propagate depends on the square root of the slope of the stress-strain curve (which, as noted, is nonlinear for most graphites). Accordingly, sound speeds computed on a basis of the initial elastic modulus (at stress levels below 750 psi, usually) are high when compared to those measured where the stress amplitude of the disturbance is two or three thousand psi.

Table I. Mechanical Properties of Graphitic Materials at Room Temperature

Material	Density $\rho$ (g/cc)	Elastic Modulus $E \times 10^{-6}$ (psi)	Sound Velocity $c_o \times 10^{-4}$ (in/sec)	Static Tensile Strength (psi)	Load Orientation
ATJ	1.73 <sup>a</sup>	1.4 <sup>a</sup>	9.6 <sup>a</sup>	3000 <sup>b</sup>	Across grain
POCO	1.76 <sup>c</sup>	1.7 <sup>c</sup>	10.2 <sup>d</sup>	9000 <sup>c</sup>	---
Graphitite G	1.90 <sup>c</sup>	1.26 <sup>c</sup>	8.5 <sup>d</sup>	2500 <sup>c</sup>	Across grain
PG	2.18 <sup>e</sup>	1.37 <sup>f</sup>	8.3 <sup>d</sup>	2000 <sup>f</sup>	Across grain
Boron PG	2.21 <sup>c</sup>	1.37 <sup>f</sup>	8.2 <sup>d</sup>	3000 <sup>f</sup>	Across grain
Hafnium PG	2.50 <sup>f</sup>	5.0 <sup>f</sup>	14.7 <sup>d</sup>	5000 <sup>f</sup>	Across grain

<sup>a</sup>DiGiacomo (Ref. 6)

<sup>c</sup>Southern Research Institute (Ref. 4)

<sup>e</sup>Hershaft and Stein (Ref. 7)

<sup>b</sup>Seldin (Ref. 2)

<sup>d</sup>Calculated:  $c = (E/\rho)^{1/2}$

<sup>f</sup>Assumed value

## B. SHOCK WAVE PROPAGATION

In the present study, a dynamic load is applied to the test specimen by a stress wave, generated through the impact of a flyer bar or slug against one end of a transmitter bar. The test specimen is bonded to the other end of the bar. The initial compressive wave traverses the transmitter bar and the test specimen, reflects as a tensile wave from the free end of the test specimen, and returns through the system (Fig. 2). The material under study is thus first subjected to a compressive pulse, followed by an unloaded period, and then subjected to a tensile pulse; the unloaded period occurs during the time when the transmitted compressive wave and the reflected tensile wave cancel each other, as shown in Fig. 2. For the present experiments, the compressive and tensile pulses in the test specimens have a duration on the order of 2.5  $\mu$ sec at the transmitter bar-specimen interface and about half this duration in the middle of the specimen. The amplitude of the stress wave is derived from strain measurements made on the transmitter bar near the bar-specimen interface.

To simplify the analysis, four assumptions are made:

1. The loss or decay of the stress wave between the strain gage station on the transmitter bar and the bar-specimen interface is insignificant.
2. The reflected tensile wave has the same stress as the compression wave.
3. The elastic modulus of the specimen remains constant.
4. The specimen does not fail during passage of the compressive wave.

Assumption 1 is supported by calibrations of the transmitter bars that show losses to be less than 3% of the peak strain per inch of bar traversed, for strain levels less than the apparent elastic limit. Assumption 3 implies a linear stress-strain behavior for the graphites, which may be valid only for low stress levels. Hysteresis effects due to loading first in compression and then in tension are ignored in this first-order approximation, as is the effect of stress-dependent Young's modulus (due to the nonlinear stress-strain relation) on sound speed.

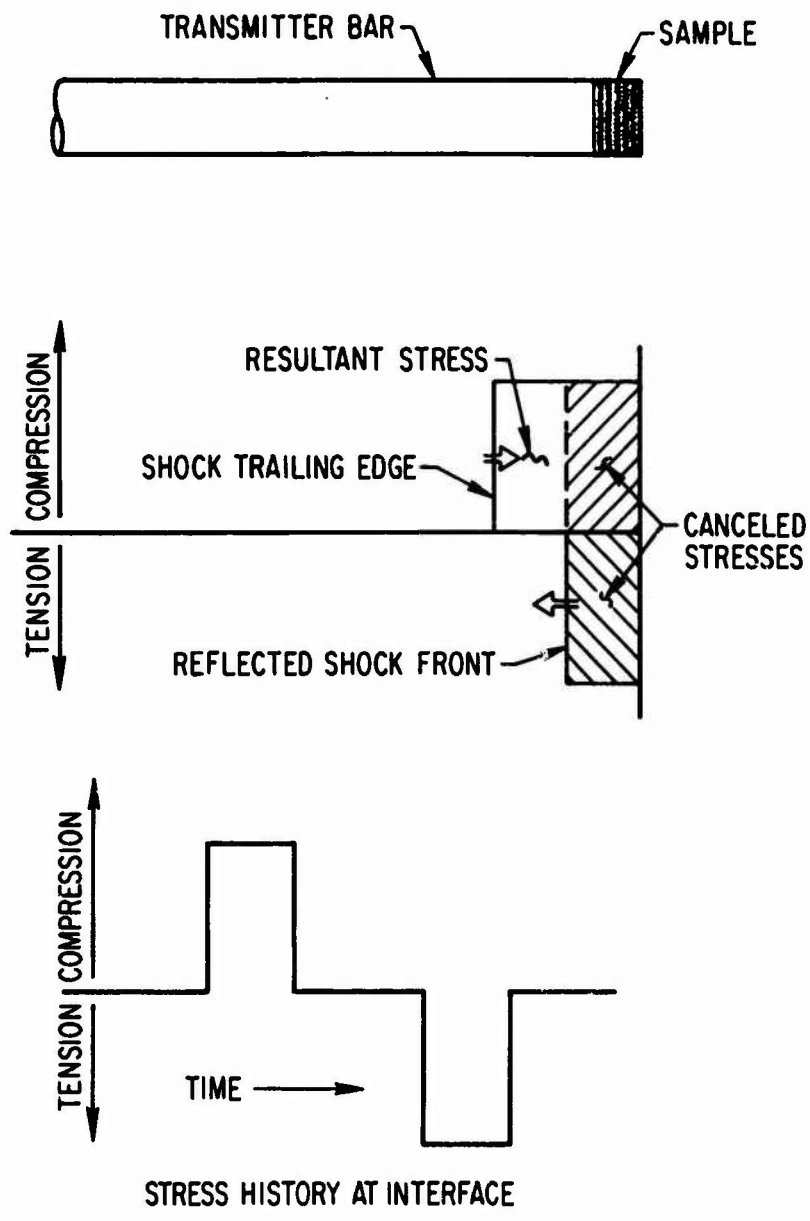


Figure 2. Tension Wave Development

During passage of the transmitted compressive wave, the particle velocities are equal across the bar-specimen interface, because of continuity requirements. For a given impact condition, the initial particle velocity  $v_1$  may be obtained from the strain measurement by the relation

$$v_1 = c_B \epsilon \quad (1)$$

where  $c_B$  is the bar sound speed for the transmitter bar material and  $\epsilon$  is the measured strain.

From conservation of momentum requirements the particle velocity ( $v_2$ ) in the sample is related to the initial particle velocity by

$$v_2 = v_1 \left( \frac{2\rho_B}{\rho_B + \frac{c_s}{c_B} \rho_s} \right) \quad (2)$$

where  $\rho_B$  and  $\rho_s$  are the density of the bar and specimen material, respectively.

The stress  $\sigma$  in the specimen is related to the particle velocity in the specimen material by

$$\sigma = \frac{E v_2}{c_s} \quad (3)$$

where  $E$  and  $c_s$  are Young's modulus and bar sound speed for the specimen material, respectively. Thus for a given impact condition, the peak stress in the specimen is obtained from the strain by the relation

$$\sigma = \frac{E c_B \epsilon}{c_s} \left( \frac{2\rho_B}{\rho_B + \frac{c_s}{c_B} \rho_s} \right) \quad (4)$$

### III EXPERIMENTAL RESULTS

The primary method, currently, of obtaining dynamic compressive properties of materials at high strain rate is by the use of the split-Hopkinson bar. Reference 8 presents data obtained by this means for a number of reentry materials, describes dynamic testing techniques, and lists additional references.

The study herein discussed is concerned with the tensile properties; however, the test apparatus is based on the same principles as the split-Hopkinson bar, except that the pressure bar used to measure the impulse after it passes through the sample has been removed. This allows the compressive wave that is propagated through the system to reflect from the free end of the sample and return through the system as a tensile wave. Figure 3 shows the experimental arrangement used to study dynamic fracture.

Dynamic tensile failure was achieved for all materials studied except for the POCO (AXF) graphite. Post-test photomicrographs of the PG-based materials, Fig. 4, show multiple delamination normal to the c-axis, as expected, in all cases. The Graphitite G material, which was loaded in the "with the grain" direction, exhibited cracking at the free surface, along a diametral line, but with the cracks initiating between layers (i. e., parallel to the direction of loading); the fracture then turned to become essentially normal to the loading direction as the crack propagated to the lateral surface of the sample. Failure of the ATJ, loaded across or "against the grain," occurred with the fracture essentially normal to the direction of loading and to the c-direction of the material (these two directions coincided). General views of typical failed samples are shown in Fig. 5.

The experimental data are given in Table II. Because fracture levels are best approached on a statistical basis, and because of the limited number of experimental data points from this study, the results in Table II have been grouped in stress loads of 1000 psi width. The last column (median fracture stress) is chiefly for use in comparing the relative performance of the various

graphitic materials. The "percent fractured" column indicates the ratio of the number of samples fractured at a given stress level (band) to the total number tested at that level. The method of determining the median fracture stress for PG is shown in Fig. 6, which also indicates typical data scatter and points out that there is no sharp division between the nonfracture and fracture stress levels.

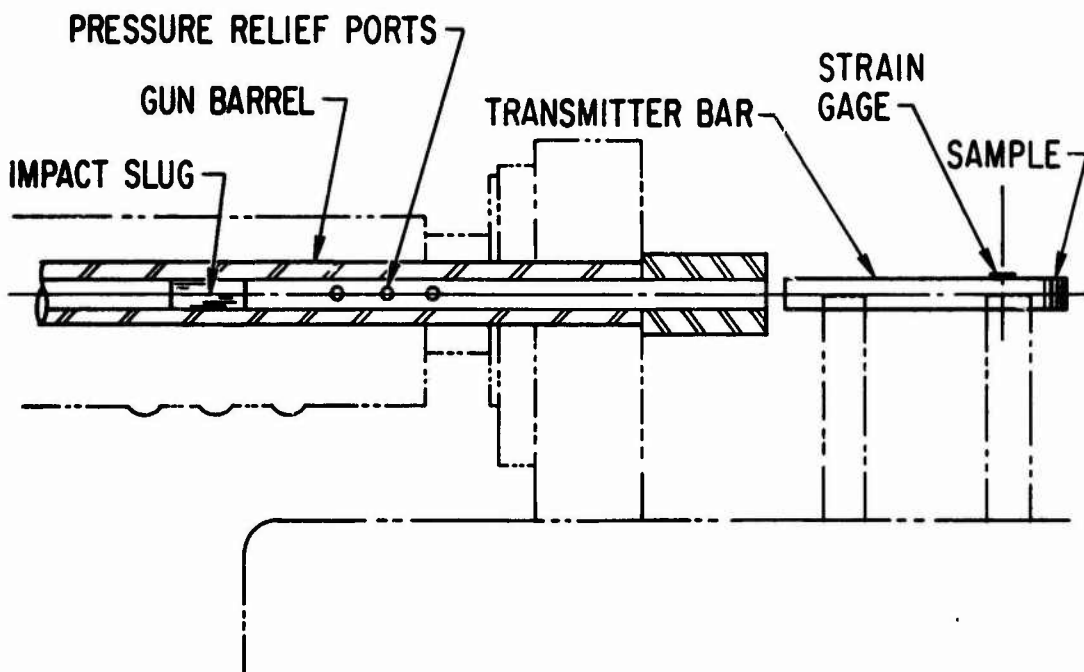


Figure 3. Test Geometry



Pyrolytic Graphite (PG)

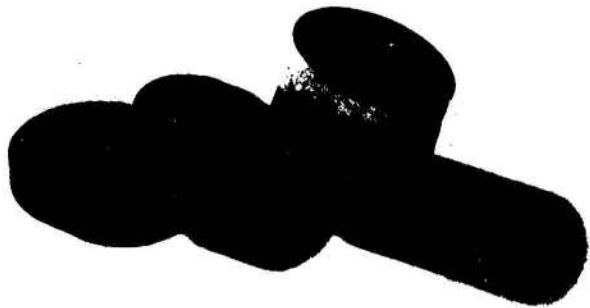


Boron-doped PG (BPG)



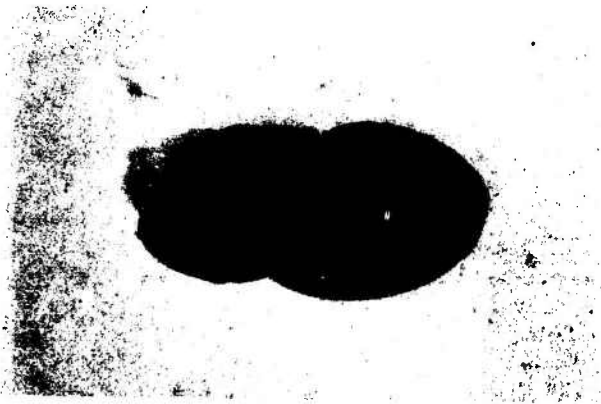
Hafnium-doped PG (HPG)

Figure 4. Post-Test Photomicrographs of Pyrolytic Graphite Materials. (c-direction is vertical. Taken  $\times 50$ ; shown  $\times 40$ .)



Note: Stress wave propagated across grain, except as noted.

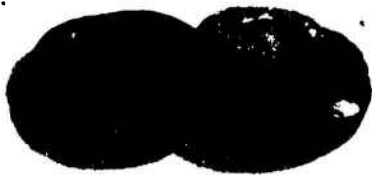
Pyrolytic Graphite (PG)



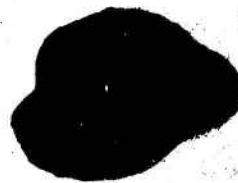
Boron PG



Graphitite G, with grain



Hafnium PG



ATJ

Figure 5. Fracture Patterns

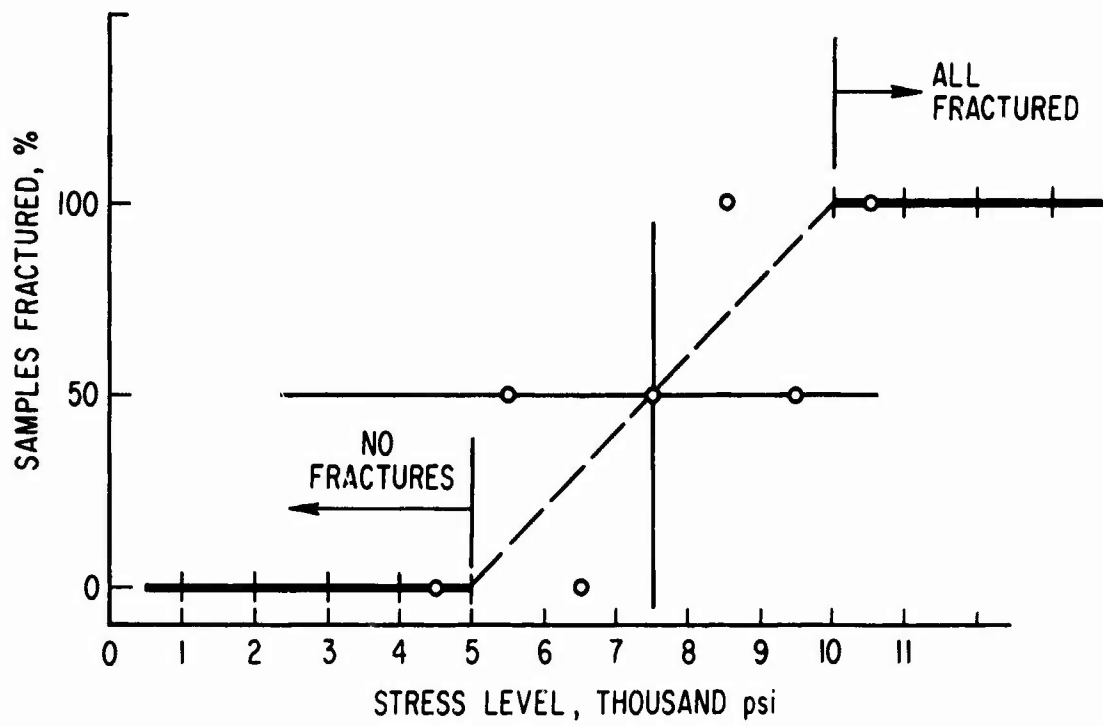


Figure 6. Determination of Median Stress for Pyrolytic Graphite

Table II. Fracture Stress of Graphitic Materials as Obtained from Impact Tests

Material	Applied Stress		Percent Fractured	Median Fracture Stress (psi)
	Nonfracture	Fracture		
ATJ	6.5, 6.5	---	0	7,000
	---	7.5	100	
	---	8.4	100	
	---	12.0, 13.4, 19.2	100	
POCO	11.0, 30.4, 34.8	---	0	>30,000
Graphitite G	2.5, 3.5, 5.0, 5.5	---	0	18,000
	13.7	---	0	
	19.0	19.0, 19.0	67	
PG	4.4	---	0	7,500
	5.6	5.6	50	
	6.3, 6.5	---	0	
	7.5	7.5	50	
	---	8.7	100	
	9.3	9.0	50	
	---	10.0, 10.0	100	
	---	11.3, 11.3	100	
	---	15.0, 15.0, 20.0	100	
Boron PG	5.5	---	0	15,000
	8.3, 8.9	---	0	
	---	11.0	100	
	13.2, 13.8, 13.8, 13.8	13.8	20	
	16.5	---	0	
	---	22.0, 27.6	100	
Hafnium PG	9.6	9.6	50	10,000
	---	12.5	0	

#### IV. DISCUSSION

The fracture surfaces of the dynamically fractured monolithic graphites are similar to, but considerably rougher than, those observed under static loading conditions (Ref. 4). The mode of failure of the Graphitite G and the ATJ materials is consistent with the hypothesis advanced in Ref. 1; fracture of the Graphitite G initiated at the free surface and in a direction parallel to the main grain orientation, so that interlayer failure could have occurred, though subsequent crack propagation eventually turned to become normal to the direction of loading. The PG-based materials failed as expected, i. e., by delamination along planes normal to the c-direction, which was also the direction of loading.

The ratio of dynamic to static tensile failure stress varies from slightly less than 2 to around 7 (Table III). These ratios are only rough indicators of relative performance, however, because of the great uncertainty that must be ascribed to the static tensile strength values employed (in addition to the qualification, discussed in Sec. III, regarding the dynamic median fracture levels in Table II). The greatest uncertainty is the static tensile strength of the hafnium PG and the boron PG; the values given in Refs. 2, 3, and 4 are believed to apply reasonably well for the remainder of the materials studied.

The Graphitite G shows the greatest increase in dynamic over static tensile strength (excluding the POCO material from consideration); this material is less porous than the ATJ materials but has a larger grain size. Shock attenuation effects might be expected to be greater and could account for the improved performance under dynamic loading. The dynamic behavior of the boron-doped PG is superior to that of the undoped PG; the apparent improvement in dynamic performance, as compared to static loading, must be taken with some reservation, however, because of the uncertainty in the boron PG static strength level, as noted above. Smaller improvements are shown in the dynamic strength of the HPG and ATJ graphites.

Table III. Comparison of Static and Dynamic Tensile Strength

Material	Density (g/cc)	Tensile Strength (psi)		$\frac{\sigma_{\text{Dynamic}}}{\sigma_{\text{Static}}}$
		Static	Dynamic	
ATJ (AG)	1.73	3,000	7,000	2.3
POCO	1.76	9,000	> 30,000	> 3.3
Graphitite G (WG)	1.90	2,500(AG)	18,000	7.2
PG (AG)	2.18	2,000	7,500	3.8
Boron PG (AG)	2.21	3,000	15,000	5.0
Hafnium PG (AG)	2.50	5,000	10,000	2.0

## V. CONCLUSIONS

Dynamic tensile properties of a number of monolithic and pyrolytic graphite materials have been obtained; in all cases, improvements over the published static tensile strength have been observed, by factors ranging from 2 to 7. The material failure modes are similar to those observed for fracture under static loading conditions. Further refinements in analysis techniques and better statistical data are required for improved understanding of the experimental results.

## REFERENCES

1. O. D. Slagle, "Deformation Mechanisms in Polycrystalline Graphite," J. Am. Ceram. Soc. 50, 495-500 (1967).
2. E. J. Seldin, "Stress-strain Properties of Polycrystalline Graphites in Tension and Compression at Room Temperatures," Carbon 4, 177-191 (1966).
3. P. Vallianos, Compressive Properties Graph-I-Tite G, PIR. No. U-8155-1171, Missile and Space Div., General Electric Co., Philadelphia (29 July 1966).
4. A Study of the Effects of Purification on the Tensile Properties of Several Graphite Materials, Final report to Aerospace Corp. 8608-1759-II, Southern Research Inst., Birmingham, Alabama (21 July 1967).
5. J. R. Cost, K. R. Janowski, and R. C. Rossi, Elastic Properties of Isotropic Graphite, TR-0158(3250-10)-13, Aerospace Corp., El Segundo, Calif. (January 1968).
6. A. F. DiGiacomo, Experimental Method of Determining the Velocity of Sound in Graphite, TDR-269(4240-30)-6, Aerospace Corp., El Segundo, Calif. (April 1964).
7. A. Hershaft and E. Stein, RADS Material Data Handbook, BSD-TR-66-372, Vol V, Avco Corp. (September 1966) (S).
8. C. J. Maiden and S. J. Green, Response of Materials and Structures to Suddenly Applied Stress Loads (Phase I), DASA Report No. 1716, General Motors Defense Research Lab., Santa Barbara, Calif. (October 1965).

UNCLASSIFIED

Security Classification

DOCUMENT CONTROL DATA - R&D		
<i>(Security classification of title, body of abstract and indexing annotation must be entered when the overall report is classified)</i>		
1 ORIGINATING ACTIVITY (Corporate author) Aerospace Corporation El Segundo, California		2a REPORT SECURITY CLASSIFICATION Unclassified
		2b GROUP
3 REPORT TITLE THE DYNAMIC RESPONSE OF GRAPHITIC MATERIALS		
4 DESCRIPTIVE NOTES (Type of report and inclusive dates)		
5 AUTHOR(S) (Last name, first name, initial) Schmidt, August E., Jr.		
6 REPORT DATE 69 MAR 25	7a. TOTAL NO. OF PAGES 23	7b. NO. OF PAGES 8
8a. CONTRACT OR GRANT NO. F04701-68-C-0200	9a. ORIGINATOR'S REPORT NUMBER(S) TR-0200(4250-30)-2	
b. PROJECT NO.		
c.	9b. OTHER REPORT NO(S) (Any other numbers that may be assigned this report) SAMSO-TR-68-380	
d.		
10 AVAILABILITY/LIMITATION NOTICES This document is subject to special export controls and each transmittal to foreign governments or foreign nationals may be made only with prior approval of SAMSO ( <del>SECRET</del> ). The distribution of this report is limited because it		
11. SUPPLEMENTARY NOTES SMSD.	12. SPONSORING MILITARY ACTIVITY Space and Missile Systems Organization Air Force Systems Command Los Angeles, California	
13 ABSTRACT Dynamic tensile properties of monolithic (ATJ, POCO (AXF), and Graphitite G) and pyrolytic graphite (PG, boron-doped PG, and hafnium-doped PG) have been obtained. In all cases, the dynamic tensile strength is 2 to 7 times the published values of static tensile strength. Material failure modes are similar to those observed for fracture under static loading conditions.		

**UNCLASSIFIED**

**Security Classification**

14

KEY WORDS

**Dynamic Tensile Strength  
Graphitic Materials  
High Strain Rate  
Wave Propagation**

**"10. (Cont.)"**

**contains technology restricted by mutual security acts.**

**UNCLASSIFIED**

**Security Classification**